SURFACE ADJUSTMENT OF THE IRAM 30m RADIO TELESCOPE

D.Morris[*], M.Bremer, G.Butin, M.Carter, A.Greve, J.W.Lamb[†],
B.Lazareff, J.Lopez-Perez[‡], F.Mattiocco, J.Penalver, C.Thum
Institut de Radioastronomie Millimetrique (IRAM)
300 Rue de la Piscine
38406 St. Martin d'Heres
France

April 29, 2008

Abstract

The techniques used to set and stabilize the surface of the IRAM 30m radio telescope to a final rms accuracy of about $50\mu m$ are described. This involved both phase retrieval and phase coherent holography using a variety of radiation sources at several frequencies. A finite element model was utilized in improving the temperature control system for the telescope structure. The factors influencing the ultimate surface accuracy are discussed.

1 INTRODUCTION

The purpose of this paper is to describe the measurement and adjustment campaign for the setting of the surface of the IRAM 30m radio telescope [1, 2], which is located on Pico Veleta, at an elevation of 2900m in southern Spain. The original specification for the surface accuracy called for a root mean square error of $100\mu m$ to enable good operability in the 3mm atmospheric window and acceptable performance in the 1.3 mm window. However there was continuing interest in improvements to enable good observations at shorter wavelengths. The campaign began in 1985 and ended with the failure of the ITALSAT F1 satellite in January 2001. The final state of the surface so achieved and its response to the environment are described.

[*]Raman Research Institute, Bangalore 560 080, India
[†]OVRO, California Institute of Technology, Big Pine, CA 93513, USA
[‡]OAN, Centro Astronomico de Yebes, Apartado 148, E-19080 Guadalajara, Spain

2 A SHORT HISTORY

The first setting of the paraboloid surface was by the classical method using an invar steel measuring tape and a theodolite [3]. This was done at an elevation 90 degrees, followed by a theoretical correction for gravitational deformations to 50 degrees - judged by the designers to be about the optimum "rigging" angle for astronomical observations. This correction, supplied by the manfacturer , was derived from a finite element model of the telescope structure.

Then followed a phase coherent holography session at 22 GHz using the Orion water vapour maser radiation [4]. During the first observations the source was in an intense outburst phase, and the signal-to-noise ratio allowed maps of 32x32 pixels to be made and a limited improvement in surface accuracy was possible. In particular measurements were made in the elevation range 40-48 degrees so that no allowance was needed for any gravitational deformations. However the signal strength rapidly dropped and became too weak for use.

Further progress was then attempted by phase retrieval holography at various frequencies in the range 86-97 GHz, using a ground based transmitter in the near field on Pico Veleta at 2.7 km distance. The astronomical (Schottky mixer) receiver was used at the secondary focus together with the standard astronomical data acquisition system. Although much higher resolution maps could be made much faster, progress stagnated around a surface accuracy of about 70 micrometers (μm). Since the measurements were made at an elevation of 11 degrees, it was necessary to correct them to 45 degrees, using the theoretically predicted gravitational deformations of root mean square (rms) $55\mu m$ at the extremes of the elevation range. Doubts remained about the accuracy of these predictions - estimated by the manufacturers as ± 20 %. There were also suspicions that the telescope surface was time variable and it was considered that faster observations were needed to check on this possibility.

At this time (1991) the geostationary satellite ITALSAT 1F, equipped with a 39 GHz beacon, became available at elevation 43 degrees. This is sufficiently close to the optimum "rigging" elevation that no correction for gravitational deformation would be necessary. It was further expected that smaller scintillation would be found over an atmospheric path at high elevation. Hence phase retrieval holography was made, again at the secondary focus, using an existing but retuned VLBI receiver. However no perceptable reduction in surface error was achieved and there was evidence of instability in the telescope surface. The measurement precision was limited by the speed and dynamic range of the astronomical data acquisition system, together with the limited signal-to-noise ratio available with the VLBI receiver. Hence a new dedicated receiving system using phase coherent holography at the prime focus was constructed.

Independent verification of a time variable astigmatism was obtained in 1993 from ellipticity measurements of defocused beam scans [5]. A series of planets were observed at 2 and 3mm wavelength, and as expected from the design of the telescope backup structure, no changes in astigmatism with elevation were detected. During the same period a parallel campaign of monitoring and improvements in the temperature control system were also instigated. Temperature sensors (164) were installed in the backup structure and yoke, and predictions of any temperature induced deformations were made by a finite element calculation. The first modification in September 1999 consisted in improved air circulation in the yoke structure which is the interface between the paraboloid and the elevation axis. Although this decreased the variations in the astigmatism predicted by the finite element model, the mean value was actually increased, almost doubled ! The second modification (October 2002) improved the temperature uniformity and control in both the backup structure and the counterweights. This further reduced the variations in astigmatism (to $8\mu m$ rms amplitude), and importantly for night time observations, reduced the mean astigmatism, calculated from the finite element model, to negligible values [6]. For example during a 5 day period of good weather in October 2002 the mean astigmatism amplitude was about $10\mu m$, with an extreme range $5 - 25\mu m$, at night time. The corresponding maximum daytime value, in sunshine, was $35\mu m$.

With the demise of ITALSAT 1F, trials of near field coherent holography were made using a transmitter mounted on Pico Veleta. Initial trials in 1998 were promising (see Figure 1), but in subsequent years time variable horizontal fringes, due to variable ground reflections, made most of the maps unusable.

A summary of the results appears in Table 1. The second column (aperture

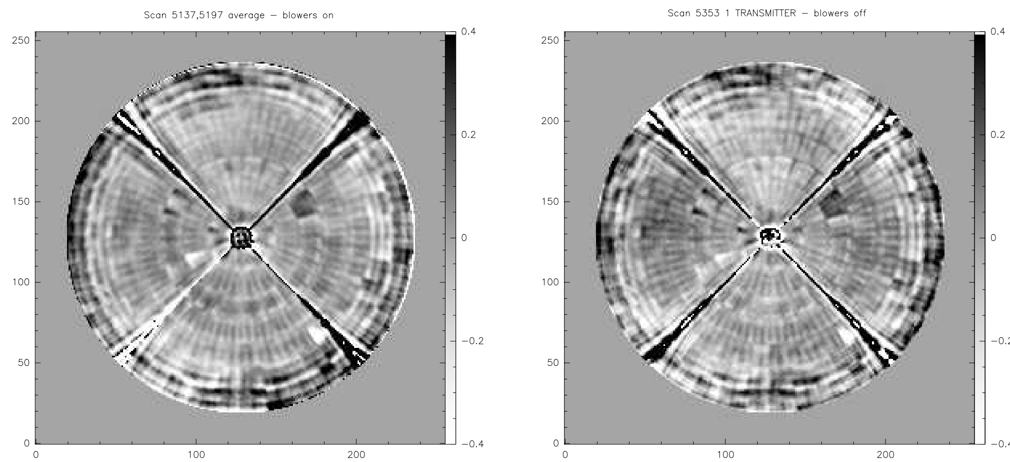

Figure 1: Aperture plane phase distributions from far field measurements using ITALSAT, 9 September 1998 (left) and from near field measurements using a 39 GHz transmitter (right) , 12 September 1998. Astigmatism fitted and removed, range of phase plotted $\pm$ 0.4 radians. A displaced test panel can be seen in the right hand quadrant. The ripples on the outer panels are due to scattering at the prime focus box.

rms error) gives the rms deviation of the aperture plane phase maps, weighted by the aperture amplitude, and expressed in μm by multiplication by $\frac{\lambda}{4\pi}$ where λ is the wavelength. Thus values are axially resolved surface error, if expressed as normal deviations from the best fit paraboloid they would be approximately 11 per cent higher (the theodolite results are such rms deviations normal to the best fit paraboloid). Values within parentheses are after fit and removal of astigmatism. When the telescope is operated at the secondary, Nasmyth, focus then additional phase errors occur due to manufacturing errors in the secondary mirror ($15\mu m$ rms) and in the Nasmyth mirrors ($10\mu m$ rms overall) and these have been included where necessary. Thus the values tabulated refer to secondary focus operation and can be used directly in the Ruze formula [7] to estimate the aperture efficiency. It should be noted that the early results are optimistic since their resolution is inadequate to resolve fine structure in the surface panels.

TABLE 1

HISTORY OF THE SURFACE ADJUSTMENT OF 30M TELESCOPE.

[rms values in μm, axially resolved]

DATE	APERTURE RMS	RMS ERROR	NUMBER SAMPLES	METHOD +FOCUS	COMMENTS
6/1984			900	Theodolite	Assembly
7/1984	145 ‡		900	Theodolite	Optical
8/1985	77	25	32x32	Coher 1 †	22 GHz Orion
08/1990	68*	25	128x128	Retr 2 ¶	96 GHz TX
3/1994	78(77)	20	64x64	Retr 2 ¶	ITALSAT
9/2000	56(47)	9(7)	128x128	Coher 1 †	ITALSAT

* In this case only corrected for predicted gravitational deformations of the backup structure to refer values to elevation 45 degrees (no allowance for panel deformations).

( ) values within parentheses are after removal of astigmatism.

‡ Normal to paraboloid surface.

¶Phase retrieval holography at secondary focus.

†Phase coherent holography at primary focus.

3 INITIAL SETTING

The reflecting surface of the paraboloid is made of 420 aluminium honeycomb panels arranged in 7 concentric rings. Their thickness is 4 cm and they are supported in pairs on 210 rigid steel frames, of depth typically 60 cm, whose average temperature is controlled by air of adjustable temperature circulating in the backup structure. The position of the focus package is stabilized by control of the temperature of its 4 (steel) support legs - in this case by circulating fluid (glycol). Adjustment of the surface can only be made using the 4 screws (5 in rings 1 and 3), which attach each of the 210 frames to the telescope backup structure (total 900 screws). The amount of the adjustment was measured by a dial gauge, electronic in later years (Figure 2). With care a setting precision of about $10 - 15\mu m$ could be attained.

Figure 2: Adjustment of the panel frames by G.Galvez. The bolt (labelled 10) supporting the panel frame, and the electronic dial gauge are visible.

4 PHASE RETRIEVAL HOLOGRAPHY (86 GHz)

This was made at the Cassegrain focus and initially used the standard astronomical Schotty mixer receiver and data acquisition system. A low power transmitter was installed in the refuge on Pico Veleta at a distance of 2.701 km (measured by GPS) and elevation 11 degrees [8]. This system suffered from poor signal-to-noise ratio and small dynamic range, and over the years was replaced with a narrow band IF system (7.5 kHz) with linear detector and faster analogue voltage to digital converter. In later years a high power Gunn oscillator was used. In all cases vertical linear polarization was used. This gave signal-to-noise ratio estimated as about 70 dB on boresight where the (power) scintillations were in the range 0.24-4.9 %.

A pair of maps with different focus settings (offsets from nominal focus of 0 and 25mm) and of 128x128 pixels could be made in 6 hours. They were made as azimuth scans separated by 20 arc seconds in elevation and sampled at $0.83\frac{\lambda}{D}$ where D is the telescope diameter. The sample time was 300 milliseconds. Such beam maps were analysed by the Misell algorithm [9] to give aperture plane maps of amplitude and phase. Near field corrections were made as a simple quadratic Fresnel correction to the aperture phase. These are believed to be in error by less than $1\mu m$ [10].

5 PHASE RETRIEVAL HOLOGRAPHY (39 GHz)

Phase retrieval holography was done between 1992 and 1995 using the 39.592 GHz beacon on the geostationary satellite ITALSAT 1F. Predictions of the satellite position as a function of time were supplied by Calfapietra of Nuovo Telespazio at the ITALSAT control center. The apparent small elliptical orbit was fitted by 3 term (4 parameter) Fourier series in azimuth and elevation. The coefficients were then used by the telescope drive program. Measurements were made from the secondary focus using an existing but retuned 43 GHz VLBI receiver. Circular polarization was used to match that of the satellite signal. The prime focus equipment box is actually of larger diameter (2.3 m) than the subreflector (2 m), and it was found necessary to cover the exposed surface of the box surrounding the mirror, with absorbing material. Otherwise an irregular ring shaped sidelobe of diameter about 1 degree and peaks of about -40 dB could perturb the beam patterns. The ring was just detectable in the extreme corners of the 86 GHz maps and did not significantly affect the 86 GHz phase retrieval measurements. The Misell algorithm has a certain rejection of such features which do not behave correctly when the telescope is defocussed and they remain in the residuals and do not appear in the solution. Since December 2000 the reflecting surface of the focus box has been inclined 20 degrees into a conical shape. Any resulting sidelobe is calculated to occur at about 3.5 degrees from boresight.

An improved linear detector with narrow bandwidth (2 kHz) at 5 kHz, set by an active filter and intermediate frequency (10 MHz) crystal filter, was used. Its linearity was measured to be better than 1% over an 80 dB range. The data acquisition used a faster (2 MHz maximum) analogue to frequency converter and counter so that a higher dynamic range could be recorded in a shorter sample time. Even so two 64x64 pixel maps, infocus and defocussed by 7mm, needed about 6 hours of observing time. Data was taken at a sampling interval of

$0.85\frac{\lambda}{D}$. Test observations made at half this interval showed that no systematic errors were incurred in this way. An infocus, on boresight, signal-to-noise ratio of 70 dB was measured on the recorded maps. This was judged enough to ensure that atmospheric variations limited the measurement accuracy. Typically one pair of beam maps yielded measurement errors of $30 - 40\mu m$. It became clear in 1995 from studying a series of smaller maps that the surface profile of the telescope could change on a time scale of 1 hour. The best surface achieved was about $77\mu m$ rms with a measurement reproducibility of about $20\mu m$.

The performance of the phase retrieval technique was checked by comparing phase retrieval maps taken in late 1995 (64x64 pixels) with phase coherent results a year later, at a higher resolution (128x128 pixels). Figure 3 illustrates the relative performance. Some differences are expected due to the known long term changes in reflector profile due to sucessive surface adjustments and environmental effects. However the difference in spatial resolution is striking - it is apparently greater than the factor 2 which would be expected. Using the phase retrieval data it would be very difficult to correct for the tilted panels of ring number 4 for example (counting outwards from the center of the paraboloid, the central blocked area being zero). It is not clear if this lack of resolution can be attributed to the random motion of the focus during the measurements (see Figure 5), or to possible environmental induced changes.

6 PHASE COHERENT HOLOGRAPHY (39 GHz)

The phase coherent holography at 39 GHz was made in the period 1996 - 2000.

6.1 39 GHz RECEIVING SYSTEM

The design of the coherent holography system has been outlined by Lamb [11, 12] and the detailed design and construction of the receivers was described by Mattiocco [13]. The system was designed to use the 39.592 GHz beacon on the ITALSAT 1F satellite. The requirements were for high surface resolution, at least 100 independent measures across the telescope diameter in as short a time as possible, given the sensitivity available.

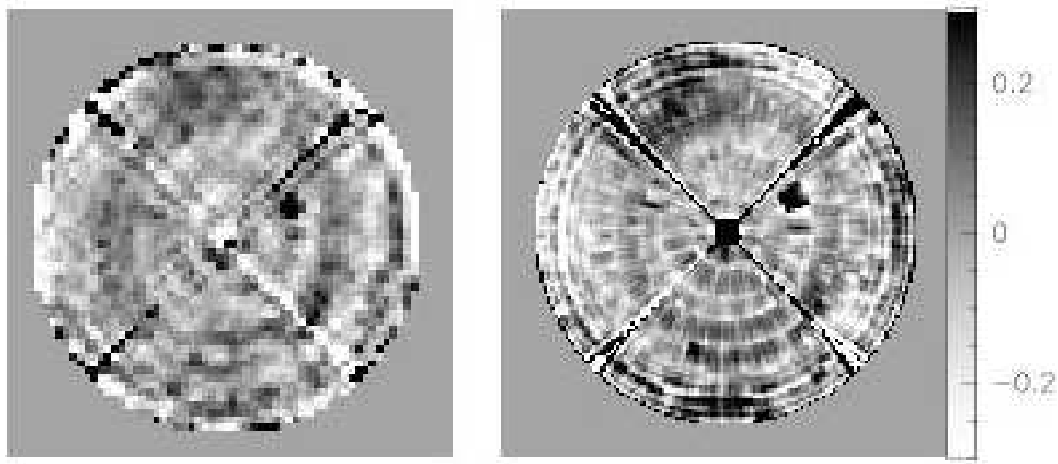

Figure 3: Comparison of phase retrieval map (left 64x64 pixels observed November 1995), with a phase coherent map (right 128x128 pixels observed September 1996). Phase range plotted ±0.3 radians (±180μm).

The receivers were mounted at the prime focus in place of the secondary mirror, (so consequently the measurements can give no information on the precision of the latter and its contribution to the overall errors). A reference signal was provided by a conical horn-lens combination of diameter 30cm, half power beamwidth 1.96 by 1.65 degrees, which "looked" forward directly along the telescope axis to the satellite through a radome at the back of the prime focus cabin. Hence even in the absence of a correction for its finite beam, the amplitude taper for a maximum scan of 1.6 degrees was only 0.84, and at least 100 essentially independent measurements were possible across the telescope aperture. The signal from the main paraboloid came from a flanged waveguide feed mounted at the prime focus. Its phase and amplitude radiation pattern were measured in an anechoic chamber at IRAM. They are believed to be accurate to better than 1 degree (equivalent to 10μm surface error). It was necessary to cover the area surrounding the feed with absorber - otherwise spurious phase ripples were produced near the edge of the aperture plane maps. Both feeds were circularly polarized to match the satellite signal (right hand).

The receiver chains for both signal and reference waveforms comprised room temperature Schottky mixers (Trx=1200 K) followed by intermediate frequency

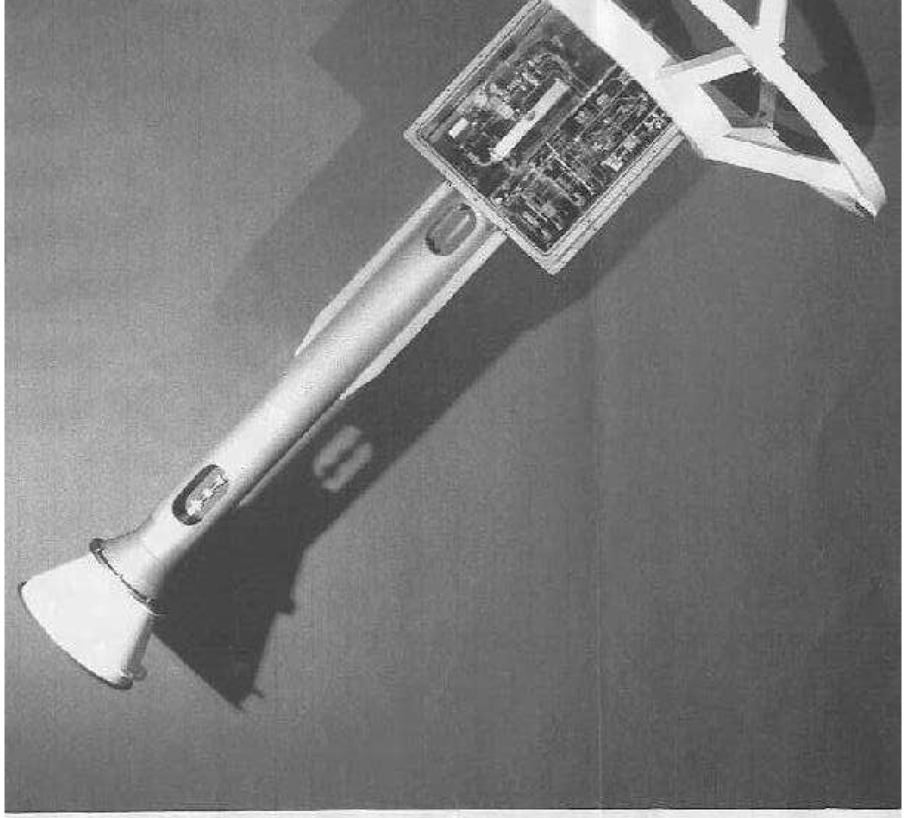

Figure 4: The "insert" comprising the two 39 GHz receivers and their feeds.

(IF) amplification at 150 MHz, 10.7 MHz and finally at a baseband of 5 kHz. The bandwidth was set at 3 kHz by crystal filters at 10.7 MHz. The long cables separating the prime focus package and the correlator in the control room carried the IF signals at 5 kHz - thus minimizing any phase errors. The local oscillator consisted of a phase locked dielectric resonator at 13 GHz followed by a tripler. The frequency reference was a low phase noise quartz oscillator. The first stages of the two receivers and their common local oscillator, and the two feeds were built as a single rigid phase stable "insert" for the prime focus (Figure 4).

Cross coupling between the two receiver chains was kept to negligible values (< -80 dB) by careful filtering and the judicious use of circulators in the local oscillator connections. The two waveforms at 5 kHz were fed to an HP 35670A digital spectrum analyser in the control room for correlation. This analyser first digitized the two waveforms and made an FFT to derive their spectra. At this stage an automatic frequency correction could be made for any Doppler effects before multiplication to derive the cross spectra. The amplitude and phase of the correlation were then derived by integration over a 4 Hz window around the peak. The analyser was controlled by a PC which stored the data and provided interrupts to the VAX telescope control computer so that analyser data and telescope position information could be merged offline later. The maximum rate at which data could be recorded was 4 samples per second.

6.2 ATMOSPHERIC EFFECTS

Atmospheric turbulence is believed to be a factor limiting the measurement accuracy. We tried to estimate the potential errors by monitoring the intensity scintillations on boresight, and also the angle of arrival fluctuations - by tracking the radiation source at the half power point of the infocus beam. This also serves to check the tracking performance of the telescope. However we found no convincing way of predicting favourable meteorological conditions, other than night-time when the turbulence was a minimum, and in very dry conditions ($\leq 5\%$ relative humidity).

6.3 RESULTS

The majority of observations consisted of 128x128 pixel maps made by scanning in azimuth at a series of elevations separated by $0.85\frac{\lambda}{D}$. Each map took 3 hours. Between each azimuth scan integrations were made on boresight for phase and amplitude calibration and adjustment for the variable Doppler shift.

A check on the tracking was usually made at the centre of the map. The root mean square pointing errors were typically of the order of 1 arc second - estimated to contribute a surface error of about $10\mu m$.

The initial test observations in 1996, made by tracking the satellite on boresight, revealed unexpected phase changes. Every 100 seconds an apparently random phase change of up to 20 degrees (equivalent to $200\mu m$ surface displacement) occurred, superposed on a saw-tooth oscillation of peak to peak amplitude 5 degrees, and period about 25 minutes - see Figure 5 (left). The phase jumps were rapidly found to be due to noise in the position readout for the servo controlling the focus package which was quickly rectified. After correcting this problem, Figure 5 (right hand plot) shows the residual oscillation due to on-off cycling of the temperature control system of the focus support legs. It was slow enough to be removed during the phase calibration of each azimuth scan. Since 2005 these

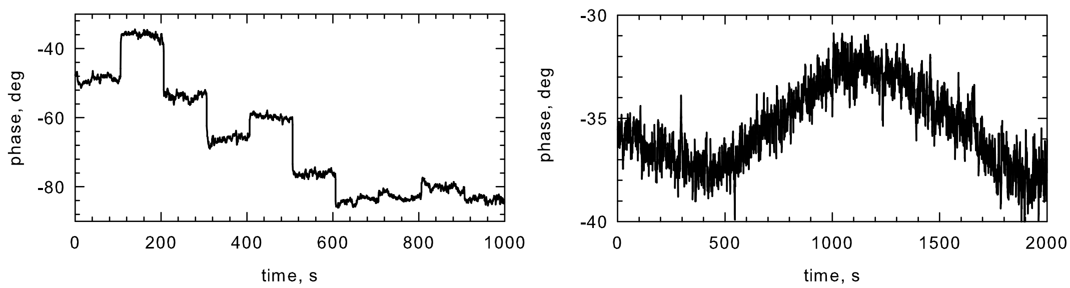

Figure 5: Periodic jumps in boresight phase due to rounding errors in the servo controlling the position of the subreflector (left), and phase variation resulting from temperature cycling of the focus support legs.

effects have been reduced by a new digital temperature controller for the circulating fluid in the focus supprt legs. Any residual length change in the legs is compensated by an automatic motion of the focus package.

However both effects were probably present during the previous phase retrieval measurements, which although disturbed could not detect and compensate for such limitations to their accuracy ! Otherwise the root mean square phase noise was close to that expected from the system noise temperature but only at night time under the very best conditions. Usually the phase noise on boresight was dominated by scintillation, in good night conditions the rms angle of arrival fluctuations were about 1 arc second rms - and much more in daytime. These fluctuations are probably on the average smaller than found on the terrestrial line of sight to Pico Veleta. However a study of the autocorrelation function of the phase errors in the aperture plane maps has suggested about equal contributions from system noise and angle of arrival fluctuations at night time - see Figure 6. The phase errors have been taken to be the difference of two aperture plane phase distributions observed sequentially. Figure 6 displays the observed correlation coefficient derived from two typical night-time observations, together with the results of simulations for a gaussian distribution of arrival angles, uncorrelated from point to point in the far field. Although the atmospheric fluctuations cannot alone account for the form of the correlation function, the inclusion of uncorrelated noise-like contributions greatly improves the agreement between theory and observations. Thus atmospheric effects apparently account for a minimum of about 40% of the errors. The remainder being due to system noise and any artifacts with short correlation length.

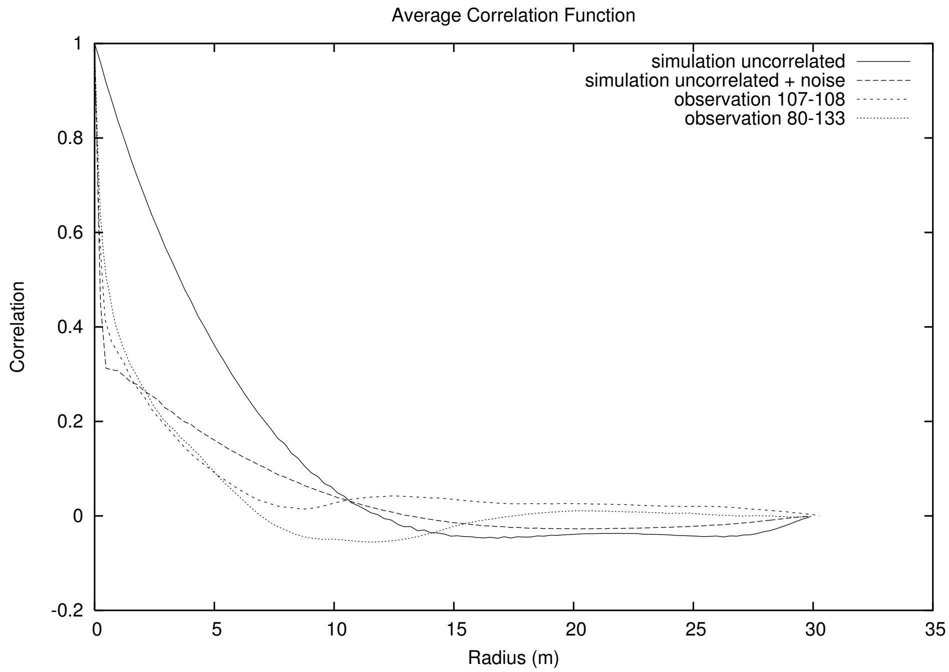

Figure 6: Autocorrelation function for aperture phase errors calculated from two pairs of aperture plane maps. They are compared with the results of simulations of angle of arrival fluctuations, with and without additional noise (full line).

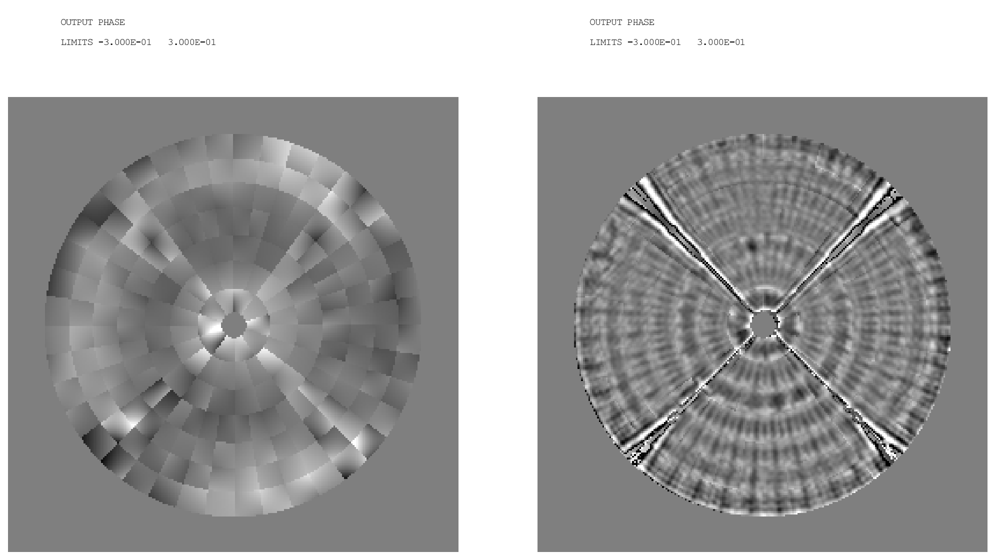

Figure 7: Least squares solution for panel settings (left) and residuals (right) for 2000 data. Range plotted ± 0.3 radians ($\pm 180 \mu m$).

Figure 6 also indicates that the atmospheric induced errors, and pointing errors, have a large correlation length, falling to zero at about 7m. This in turn has implications for the error in screw settings. If for example their correlation length were significantly smaller than the panel dimensions, they would induce a smaller error in the panel settings. These were derived by least squares fit of a panel model which gave displacement, tilts, and twist values for each panel. Throughout the holography campaign screw settings were calculated by least squares fitting of a twisted panel with four degrees of freedom, in the manner suggested by von Hoerner [14]. The screw settings were in turn calculated from these parameters. Figure 7 illustrates the results of the fit of the panels positions to the average map - taken after the last setting in September 2000. Some systematic panel alignment errors remain (left), suggesting that further improvement is possible. The residuals, also displayed (right) in Figure 7, which typically amount to about $40\mu m$ rms reveal the systematic panel errors - predominately a systematic "scalloping". This is believed to be due to manufacturing errors which were measured in the factory as $28\mu m$ rms, other contributions to the residuals come from thermal distortion of the panel frames, gravitational deformations of the panel frames, and of course the measurement errors.

Figure 8 (left) shows the "final" aperture plane phase distribution measured in September 2000 after the last surface adjustment. It is the average of 4 individual maps with any residual astigmatism removed. We estimate from their scatter that the random measurement error (reproducibility) of this average map is $7\mu m$ rms. The amplitude weighted axially resolved rms surface error of this map is $56\mu m$, $47\mu m$ excluding the astigmatism (of amplitude $107\mu m$). This latter value ($47\mu m$) thus applies to the paraboloid after the second and final improvement of the temperature control system. For secondary focus operation these numbers must be increased to allow for the surface errors of the hyperboloid ($13\mu m$ axially), and the Nasmyth mirrors ($10\mu m$).

In the absence of astigmatism this leads to $50\mu m$ rms amplitude weighted, axially resolved aperture plane error for secondary operation at elevation 43 degrees, in calm night time conditions. When the telescope surface is exposed to full noontime sun, this error is expected to rise to about $66\mu m$ due to the panel frame deformations (about $45\mu m$ rms). Of the $47\mu m$ error in the paraboloid

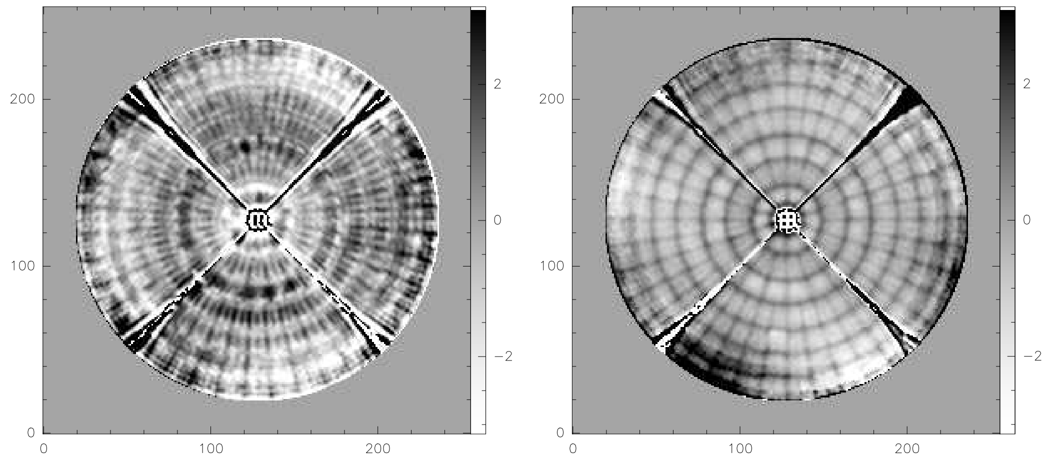

Figure 8: Left - Aperture plane map of surface error measured in September 2000 after the last adjustment. Astigmatism fitted and removed. Range plotted ± 0.2 radians (±120μm). Units for axes are pixels of 13.8 cm. Right - Surface change between midnight and noon in full sunlight. Range plotted ± 0.5 radians (±300μm).

surface about 40 are contributed by the fitting residuals so the remaining 25μm of the root sum square error can be attributed to uncorrected panel frames. This represents an additional potential improvement in the telescope performance which could be achieved by further adjustments. At best this could reduce the effective surface error for Cassegrain operation from 50μm to about 43μm.

During the period of the 39 GHz phase retrieval measurements, a parallel study of the telescope astigmatism and its origin in thermal changes of the structure was being made. As a consequence several improvements in the temperature control for the telescope backup structure were made [15, 6, 16]. However before these were completed the astigmatism was expected to be variable during the holographic measurements of 2000 and it was ignored in the surface setting by fitting and removing it from the maps of aperture phase before calculating the panel frame adjustements. Thus the surface adjustment was restricted to "polishing" the finer scale deformations. In 1998 tests were made with the temperature control system disabled to check on the reliability of the predictions of the finite element model. Figure 9 shows the correlation between measured and predicted amplitude of the astigmatism. The curve is for a surface with a constant offset of amplitude 48μm, although a fit without such an offset is equally good. In fact

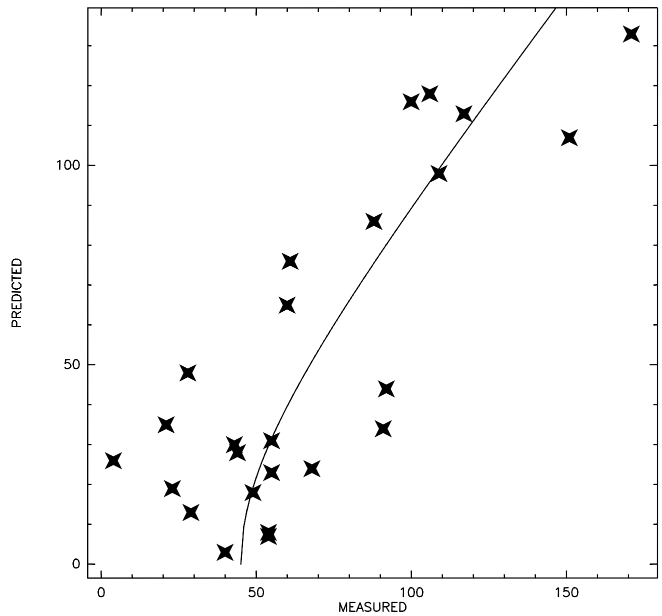

Figure 9: Comparison of astigmatism amplitude measured by holography (abscissa μm) with that predicted (ordinate) from the finite element model and the measured temperature distribution in the backup structure.

at night-time with the temperature control in operation the predictions agreed very well with the values measured by holography and any offset is believed to be negligible, see Table 2.

TABLE 2

MEASURED AND PREDICTED ASTIGMATISM AT NIGHT.

[amplitudes in μm]

DATE	OBSERVED	PREDICTED	COMMENTS
1999	51	55	Initial temperature control
2000	107	105	Improved air circulation in Yoke
2002		15 ± 5	Improved temperature control in Yoke

6.4 ENVIRONMENTAL EFFECTS - DAYTIME PERFORMANCE

Comparison of aperture plane maps taken in daytime and at night show striking effects. Figure 8 (right) shows the difference in aperture plane phase distributions between midnight and midday when the sun was about 35 degrees from boresight. During the observations this angle covered the range 29, through 10, to 42 degrees. The deformations occur on the scale of the panel frames which bulge up towards the focus at midday, and in the opposite sense, to a lesser degree at midnight. The peak to peak difference visible on Figure 8 (right) is about 0.28

radians ($168\mu m$). At midnight a typical peak to peak error of about $50\mu m$ ($16\mu m$ rms) seems likely, and in full sun illumination about $120\mu m$ peak to peak. The origin of these deformations of the panel frames was confirmed by temperature measurement on a "representative" frame. The inner tubes of the frame, furthermost from the reflecting surface, follow the temperature of the circulating air, however that part nearest the surface is approximately 1.75 degree cooler at midnight, and 2.75 degrees warmer at midday. Since the steel frame has a thickness of 60 cm perpendicular to the reflecting surface these temperature gradients are sufficient to explain a significant part of the observed distortion. A finite element model of the frame predicts a peak to peak deformation of $40\mu m$ at midday, $31\mu m$ at midnight [17] for the temperature gradient quoted above. During the holography measurements no temperature measurements of the ensemble of panel frames could be made so better agreement between predicted and observed frame deformations can not be expected.

7 CONCLUSIONS.

Since the installation of the second improvement in the temperature control of the backup structure (in 2002) the calculated astigmatism is quite negligible [6]. Hence the present surface profile is as measured in 2000 with astigmatism fitted and removed. The amplitude weighted, axially resolved, surface error at elevation 43 degrees in calm night time conditions is $47\mu m$ for prime focus, $50\mu m$ for secondary focus operations. The environmental effects (sunlight and wind) have been checked and agree quite well with predictions from finite element models. At midday in full sunlight about $66\mu m$ has been measured by holography - with prominent ring sidelobes [18]. At other elevations these values will be increased by a contribution from the gravitational deformations which increases approximately linearly to rms values of about $55\mu m$ [19, 20], at horizon and zenith. As indicated above the ultimate surface accuracy is probably $43\mu m$ for Cassegrain operation if all the panel frames can be perfectly set.

8 ACKNOWLEDGMENTS.

Thanks are due to Sr.Calfapietra of Nuova Telespazio and Dr.Marcaronici of the Italian Space Organisation for supplying tracking information for ITALSAT 1F. R.Hills gave help and advice on raytracing and phase retrieval techniques. The staff of the Yebes observatory provided orbital elements for our initial work, and help with receiver installation and observations (the late J.E.Garrido). The IRAM staff in Spain provided excellent support over many years - H.Hein, S.Navarro and D.John with hardware and logistics, W.Brunswig and J.Schraml with software, and G.Galvez for the screw adjustments. P.Raffin made a model of the telescope support structure. D.Morris thanks the director and staff of the Raman Research Institute for their hospitality and help during the preparation of the manuscript.

References

[1] Baars J.W.M.,Hooghoudt B.G.,Mezger P.G.,and de Jonge M.: 'The IRAM 30 m radio telescope on Pico Veleta, Spain', Astron. Astrophys., 1987, **175**, pp. 319-326

[2] Baars J.W.M., Greve A., Hein H., Morris D., Penalver J., Thum C.: 'Design parameters and measured performance of the IRAM 30-m millimeter radio telescope', Proc. IEEE, 1994, bf 82, (5), pp. 687-696

[3] Greve A.: 'Reflector surface measurements of the IRAM 30-m radio telescope', Int. J. Infrared and MM Waves, 1986, **7**, (1), pp. 121-135

[4] Morris D.,Baars J.W.M.,Hein H.,Steppe H.,Thum C., Wohlleben R.: 'Radio holography reflector measurements of the 30-m millimeter telescope at 22 GHz with cosmic signal', Astron.Astrophys., 1988, **203**, pp. 399-406

[5] Greve A.,LeFloch B.,Morris D.,Hein H.,Navarro S.: 'Astigmatism in reflector antennas: Measurement and correction', IEEE Trans. Antennas and Propagation, 1994, **AP42**, pp. 1345-1350

[6] Greve A.,Bremer M.,Penalver J.,Raffin P.,Morris D.: 'Improvement of the IRAM 30-m telescope from temperature measurements and finite element

calculations', IEEE Trans. Antennas and Propagation, 2005, **AP53**, pp. 851-860

[7] Ruze J.: 'Antenna tolerance theory - a Review', Proc. IEEE, 1966, **54**, pp. 633-640

[8] Morris D.,Hein H.,Steppe H.,Baars J.W.M.: 'Phase retrieval radio holography in the Fresnel region: Tests on the 30m telescope at 86 GHz', IEE Proc. H,1988, **135**, (1), pp. 61-64

[9] Misell D.L.: 'A method for the solution of the phase problem in electron microscopy', J. Phy. Appl. Phys., 1973, **6**, pp. L6-L9

[10] Morris D,: 'Errors in near-field radioholography', IET Microw. Antennas Propag., 2007, **1**, (3), pp. 586-591

[11] Lamb J.W.: 'Sensitivity considerations for holography receiver', Internal Report, (IRAM 9 March 1995)

[12] Lamb J.W.: 'Data acquisition for phase-coherent holography', Receiver Technical Memo No.8, (IRAM, 15 October 1996)

[13] Mattiocco F.,Cocher P.M.,Bortolotti Y.: '39.592 GHz holography dual channel receiver user's manual', Receiver Technical Memo No.6, (IRAM, March 1996)

[14] von Hoerner S.: 'Internal twist and least squares adjustment of four-cornered surface plates for reflector antennas', IEEE Trans. Antennas and Propagation, 1981, **AP29**, (6), pp. 953-958

[15] Bremer M.,Penalver J.: 'FE model based interpretation of telescope temperature variations', Proc. SPIE, 2002, **4757**, pp. 186-195

[16] Greve A.,Bremer M,: 'Calculated thermal behavior of ventilated precision radio telescopes', IEEE Antennas and Propagation Magazine, 2006, **48**, (3), pp. 9-19

[17] Plathner D.: 'Studies on 30m-panel frames under Thermal Gradient', Working Report No. 244, (IRAM 1997)

[18] Greve A.,Morris D.: 'Repetative radio refector surface deformations', IEEE Trans. Antennas and Propagation, 2005, **AP53**, pp. 2123-2126

[19] Brandt P. and Gatzslaff H.: 'Das design des 30-m-Millimeterwellen-Radioteleskops', Tech. Mitt. Krupp-Forsch.Ber., 1981, **39**, (H3), pp. 111-124

[20] von Hoerner S.,Wang W.Y.: 'Gravitational deformation and astigmatism of tiltable radio telescopes', IEEE Trans. Antennas and Propagation, 1975, **AP23**, (5), pp. 689-695